Long-Axis Cardiac MRI Contour Detection with Adaptive Virtual Exploring Robot

Mark Blok[1,2], Mikhail G. Danilouchkine[1], Cor J. Veenman[2], Faiza Admiraal-Behloul[1], Emile A. Hendriks[2], Johan H. C. Reiber[1], and Boudewijn P. F. Lelieveldt[1]

[1] Leiden University Medical Center, 2300 RC Leiden, The Netherlands
[2] Delft University of Technology, 2628 CD Delft, The Netherlands
mark_blok@wanadoo.nl

Abstract. This paper describes a method for automatic contour detection in long-axis cardiac MRI using an adaptive virtual exploring robot. The robot is a simulated trained virtual autonomous tri-cycle that is initially positioned in a binary representation of the left ventricle (LV) and finds the contours during navigation through the ventricle. The method incorporates global and local prior shape knowledge of the LV in order to adapt the navigational parameters. Together with kinematic constraints, the robot is able to avoid concave regions such as papillary muscles and navigate through narrow corridors such as the apex. Validation was performed on in-vivo multiphase long-axis cardiac MRI images of 11 subjects. Results showed good correlation between the quantitative parameters, computed from manual and automatic segmentation: for end-diastolic volume (EDV) r=0.91, for end-systolic volume (ESV) r=0.93, ejection fraction (EF) r=0.77, and LV mass (LVM) r=0.80.

1 Introduction

Over the last decade cardiovascular MRI imaging has become the clinical standard for the functional assessment of the human cardiovascular system. A typical MRI study consists of a large amount of data and, therefore, automated analysis of acquired data is desirable in the daily clinical practice.

For modelling and extracting myocardium borders a large number of techniques have already been proposed. For example, Active Contour Model (ACM) is a deformable contour, which is widely employed for tracing the cardiac borders [1]. Deformation is governed by the internal and external energies. The internal energy assures the contour's smoothness imposing constraints on its shape. The external energy attracts the contour to the object's boundaries. ACM comes short in segmentation of long-axis cardiac images. The contour has to be rigid enough to prevent its deformation outside the myocardial borders, where the boundaries are not well defined (e.g. boundary between the myocardium and papillary muscles or liver), and it must be flexible enough to provide reliable segmentation of regions with high curvature (apex). A technique, based on Active Appearance Models (AAM) [2] overcomes the aforementioned drawbacks of

A.F. Frangi et al. (Eds.): FIMH 2005, LNCS 3504, pp. 54–64, 2005.

ACM by incorporating knowledge about the myocardial boundaries. This knowledge is formalized in terms of the statistical properties of the average heart's shape and appearance (gray-level representation) as well as the main modes of variation found in a training set. The AAM model placed in a new image is deformed to minimize the difference between the model and object of interest within the image. The deformation is restricted to variations found in the training set. AAM's were used for extraction of the cardiac borders at end-diastole and end-systole and showed good correlation between automatically delineated and expert contours [3]. However AAM's can be successfully used to match an object with the statistically plausible shape, while it fails to recognize the object of interest that shows large deviation from shapes in the training set.

An novel method for myocardial border detection based on a virtual exploring robot was introduced in [4]. The robot is represented as a tricycle with a steering front wheel. It can automatically navigate through an environment (myocardium). Using the frontal and lateral range sensors the robot is able to detect the coordinates of obstacles (myocardial borders) and to plan a safe path towards the target avoiding these obstacles. The robot was used for short-axis contour extraction in MRI data sets and showed promising results.

In this paper we propose a new system for automatic delineation of long-axis contours for both two- and four-chamber orientations using a modified version of the robot. The navigational environment is constructed with an improved segmentation procedure based on both intensity and spatial information to reduce misclassification of pixels. The path planning is made more robust allowing the navigation in narrow regions with high curvature. The robot is made adaptive with respect to its length, speed and maximum turning angle, depending on the local LV geometry.

2 Methods

The global outline of the system is as follows. The multiphase images in two- or four-chamber view are automatically segmented by fitting finite gaussian mixture into the combined image histogram and applying spatial regularization in terms of Markov Random Field (MRF). The classified pixels are subsequently recombined to yield binary images consisting of the allowed navigational space or obstacles. For each binary image the initial start position and orientation for the robot as well as the target are determined. The navigational environment along with the robot's initial position and orientation provides the input for the next step. The myocardium is divided into four different segments. The robot is initialized once at the segment boundaries and cruises through the navigational environment until the end of the segment is reached. Depending on the local LV geometry the robot adapts its navigational parameters to prevent from getting stuck and to avoid concave regions such as the papillary muscles, collect information about the endocardial (endo) and epicardial (epi) boundary points. Finally, the detected edge segments are used to reconstruct the endo- and epi-contours.

2.1 Creation of Navigational Environment

The robot is designed to navigate through a binary environment. Therefore, the gray-level images must be converted into binary images consisting of allowed navigational space (myocardium) and obstacle (blood pool and air).

To automatically segment the image, the pixels are grouped into classes by modelling the pixel intensity distributions with three gaussian mixtures using Expectation-Maximization (EM) [5, 6] with greedy search heuristics [7]. During the expectation step the pixels are assigned to a class with the highest conditional probability based on previous estimates of the distribution parameters. In the maximization step the distribution parameters are updated to maximize the log-likelihood. These two steps are repeated until convergence.

With the estimated pixel intensity distributions the images can be segmented into blood, myocardium and air. However statistical segmentation based only on the pixel intensity may lead to misclassification due to the presence of noise. Therefore, the context of the pixel's neighborhood is taken into account and pixel intensity information is augmented with spatial regularization using MRF [8]. The amount of spatial regularization is limited to 8-connected neighborhood and pairwise interaction between two neighboring pixels. The spatial mixture model yields the final classification of the image and is schematically represented in Fig. 1.

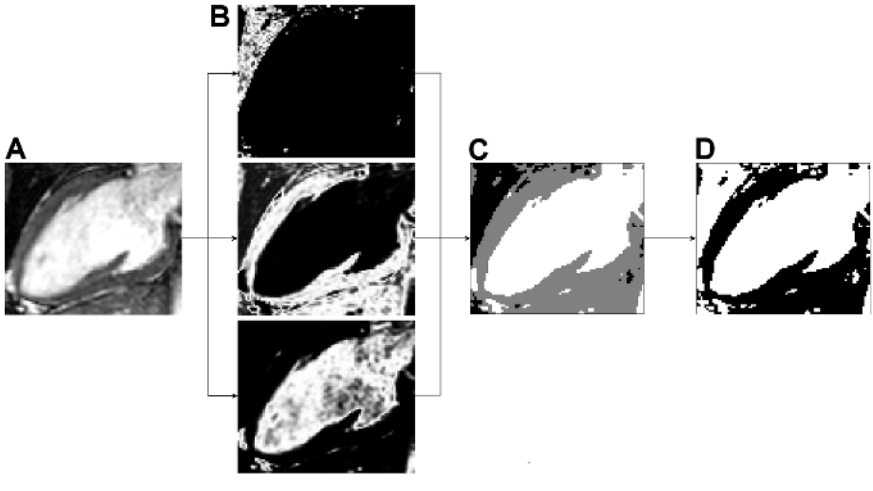

Fig. 1. Creation of navigational environment: (A) input image; (B) probability density maps for air (top), myocardium (middle), blood (bottom); (C) statistical segmentation with spatial regularization; (D) navigational environment - white corresponds to obstacle space, black - to allowed navigational space

2.2 Estimation of Initial Navigational Parameters

For the autonomous navigation in the allowed space the robot needs the starting position, starting orientation, and target. Based on the assumption that the

LV resembles a truncated ellipse at end-diastole, fitting an ellipse [9] into the myocardium gives a good approximation of the spatial orientation of the LV. Using the elliptic model the important anatomical landmarks can be localized and division of the heart into four non-overlapping segments can be done (Fig.2). The apex is located by finding the intersection point between the long axis of the ellipse and myocardium and yields the end point of the apical segments. The boundary between the basal and midventricular segments is put at the intersection of the myocardium with the line that is parallel to the ellipse short-axis and passes though the ellipse focal point, thus serves as the starting point for the robot navigation. The target is located in the ellipse center and the start orientations are the direction of the tangent line of the closest point on the ellipse. From the starting position the robot cruises through the allowed space, bounces from the endocardial LV border in attempt to reach the target and proceeds further until the end of the segments. It is initialized in each segment and navigates twice towards the mitral valve points and twice to the apex.

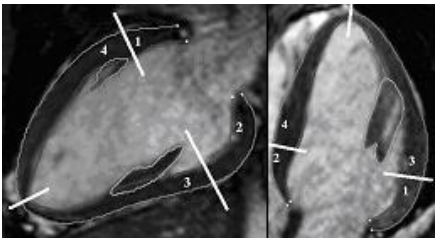

Fig. 2. Division of the LV into four segments. Segments 1 and 2 cover to the basal part, while segments 3 and 4 represent the midventricular and apical parts

2.3 Adaptive Robot Navigation

The robot is a tricycle with a front steering wheel as is illustrated in Fig.3A. The position and orientation of the robot are characterized by $p(x, y, \theta)$, where x and y are the coordinates of the front wheel, θ is the orientation of the robot with respect to the x-axis of the coordinate system, l is the length between the front and rear wheel axis, ϕ is the orientation of the front wheel. The robot moves with a constant speed v. Its motion obeys the following kinematics equations:

$$\dot{x} = v\cos(\phi)\cos(\theta); \quad \dot{y} = v\cos(\phi)\sin(\theta); \quad \dot{\theta} = \frac{v}{l}\sin(\phi) \tag{1}$$

The robot is subject to the non-holonomic constraints: it can only move along a direction perpendicular to its rear wheel axis and its maximum front wheel angle is upper bounded.

To navigate through the allowed space towards the target the robot is equipped with range sensors of a limited length (Fig.3B). The frontal sensors have their origin at the front wheel and cast rays at the different angles with

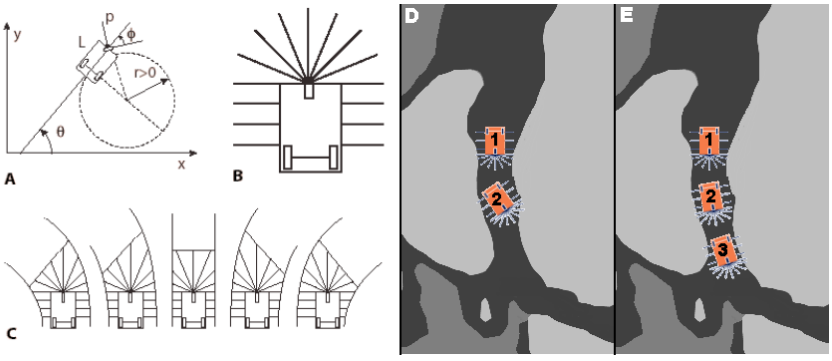

Fig. 3. The virtual mobile robot as a tricycle with the steering front wheel (A); Mounted frontal and lateral sensors (B); Navigational corridors corresponding to the different orientation of the front wheel (C); Robot navigation (D and E)

respect to the robot axis - a line connecting the front wheel and the middle point of the rear wheel axis. These sensors are primarily used to scan the environment in the vicinity of the current robot position, to detect the obstacles and to plan further movements towards the target. The lateral sensors, which are mounted on the left and right sides of the robot and perpendicular to the robot axis, are intended for inner and outer myocardial border detection.

The concept of the pre-computed corridors turns the robot navigation into a computationally efficient procedure. Depending on the orientation of the front wheel and using the kinematic equations (1) a trajectory of the robot or a corridor can be calculated. Provided that the corridor has a limited width the distances to its boundary for each range sensors can be computed and saved (Fig.3C). This procedure is repeated for each orientation of the front wheel. These pre-calculated distances are used during the navigation of the robot. While navigating, the robot scans the surrounding environment before moving forward. The range sensors give the information about the distances to the obstacle at the current robot's positions. These distances are compared to the ones of the pre-computed corridors and a decision about the corridor safety is made. The corridor is assumed to be safe if the distances to the obstacle at the current positions are bigger than the distances to the pre-computed corridor boundaries for each range sensor. Among possible safe corridors the one leading closest to the target is taken [4].

This approach to path planning was successfully applied for myocardial border delineation in short-axis images and is not robust enough for contour detection in the long-axis views. The LV geometry in two- and four-chamber projections consists of the regions with the variable myocardial width thickness and high curvature. Moreover, the information obtained from the discrete sensory system is not sufficient to reconstruct a precise topological structure of the allowed navigational space for such regions. This situation is illustrated in Fig.3D. From the initial position, marked as one, the robot moves to position two fol-

lowing the "closest safe corridor" strategy. However, being in position two the robot cannot enter the narrowing region in front of it without bumping into the obstacle and, therefore, cannot advance forward.

To solve the problem mentioned above the navigational strategy has been modified to assure its robustness in two- and four-chamber views. The basic idea is to find the safest path with a "look-ahead" procedure. The robot is allowed to explore the surroundings by advancing a number of steps in forward direction from its current position and choosing the longest and safest path leading closest to the target. After such a path has been found, the robot advances one step ahead. Fig.3E shows the path planning procedure using the "look-ahead" strategy. From position one the robot moves forward to position two, from which a safe move to position three is guaranteed due to better path planning. Therefore, the navigation through highly curved regions with the variable myocardial thickness is made more robust.

To account for the complex LV shape in two- and four-chamber views, the robot's navigational parameters are made regionally dependent. Three different regions, namely basal, midventricular, and apical, are commonly addressed in the medical literature and their geometric properties can be summarized as follows:

- Apical: high curvature with significantly changing myocardial thickness;
- Midventricular: low curvature with concave regions such as the papillary muscles;
- Basal: medium curvature of a constant myocardial thickness.

We exploit this knowledge to deduce estimates for the navigational parameters:

- Apical: The robot has to be highly mobile, which is guaranteed by its short length and slow speed.
- Midventricular: The robot is made long and fast enough to avoid the concave regions.
- Basal: The robot has a medium velocity and is made long enough to stop at the mitral valve points without a possibility of turning around.

The robustness of the robot navigation with respect to the navigational parameters has been tested in a pilot study performed on a dataset acquired from several subjects. The initial guesses for the parameters were chosen by taking into account the aforementioned considerations and analyzing the global geometric properties such as the size and maximal curvature of each cardiac segment. The final parameters, shown in Tab.1, were derived from the initial guesses by brute-force optimization.

Having been safely initialized inside the allowed navigational space, the robot autonomously explores the structure of the each myocardial segment. In attempt to reach the target, which set in the middle of the LV cavity, the robot bounces from the obstacle, formed by the LV blood pool, and proceeds further along the endocardial border. As the target is located inside the obstacle space and could not be possibly reached, the robot eventually arrives to the end of the segment and stops. During the trip the robot uses the lateral sensors to detect

Table 1. Robot's navigational parameters

Parameter	Basal Segment	Midventricular Segment	Apical Segment
Speed (mm/step)	4.17	6.59	2.78
Length (mm)	13.9	13.9	6.95
Number of corridors	15	21	19
Sensor length endo (mm)	6.95	2.78	6.95
Max steps looked ahead	1	2	2

the presence or absence of the myocardial borders (i.e.the transactions between the allowed navigational space and obstacle), and memories the coordinates of the candidate border points. This navigational procedure is repeated for all four segments, resulting in complete exploration of the left ventricle in a two- or four-chamber view.

2.4 Contour Reconstruction

The final step in automated contour detection is collecting the contour segments found by the robot and merge those together in a single contour. Reconstruction of the endo-contour is relatively straightforward. The papillary muscles are already removed due to the kinematic constraints of the robot and short lateral sensors used for endo-cardiac border detection. Therefore, connecting the detected points is sufficient to reconstruct the endo-contour. Reconstruction of the epi-contour is more challenging (Fig.4). Firstly, the outliers (falsely detected boundaries) has to be removed. To achieve this, goal prior knowledge about the myocardial thickness is used. The reconstructed endo-contour provides the reference to approximate the wall thickness. The distance between each epicardial candidate point and the reference is measured. All points, for which the calculated wall thickness is larger than a predefined threshold of 30mm, are deleted. Secondly, an additional step is required to approximate possibly missing segments caused by the absence of the myocardial border in the regions where the

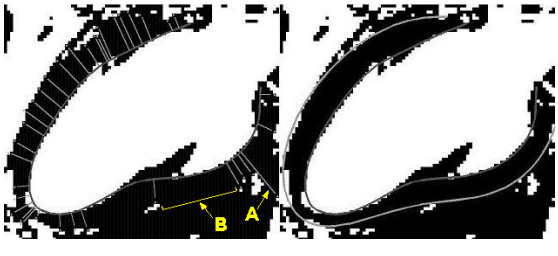

Fig. 4. Reconstruction of endo- and epi-contours (left). Prior knowledge about the myocardial wall thickness is used to remove outliers (A). The missing segments (B) are interpolated using non-uniform cubic splines. Reconstructed contours (right)

heart is adjacent to the organs with the same grey-level intensities (i.e. liver). To restore the missing information interpolation using the non-uniform cubic splines [10] is performed.

3 Results

In-vivo cardiac long-axis images were obtained at Leiden University Medical Center from 11 subjects using a Philips Gyroscan Intera 1.5T MRI scanner. Balanced-FFE protocol with prospective VCG and respiratory triggering was utilized to acquire breath-hold cardiac images in two-chamber and four-chamber views. Thirty phases provided the complete coverage of the cardiac cycle resulting in a total of 660 cardiac datasets. The field of view and slice thickness were equal to 350 mm and 8 mm, respectively. The reconstruction matrix of 256x256 was used. The total acquisition time did not exceed 10 minutes.

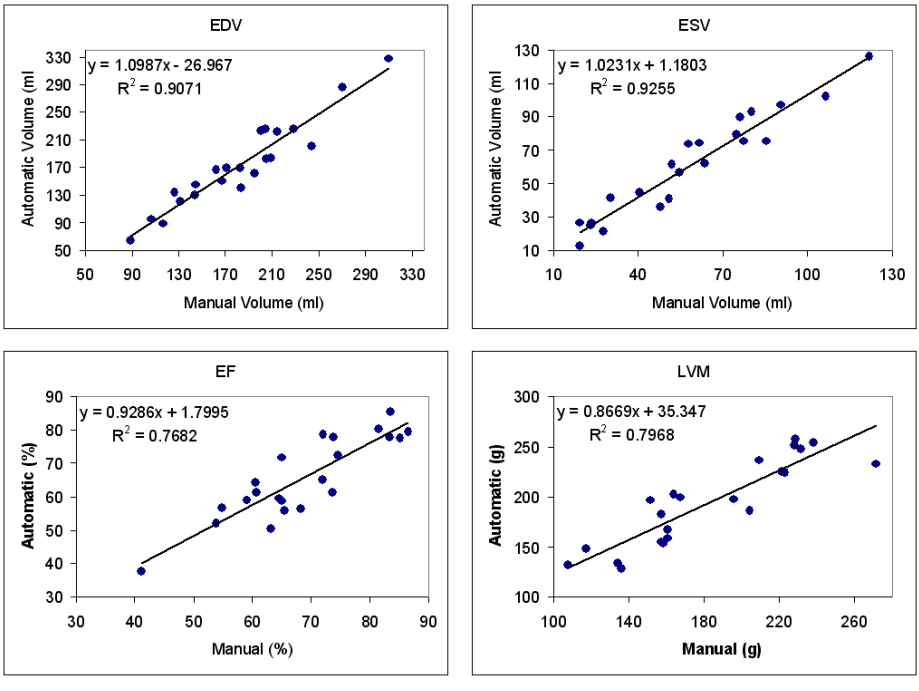

Fig. 5. Results of the statistical comparison between global LV function for manually and automatically segmented images

To assess the algorithm's performance the global LV function was computed for manually and automatically segmented images using commonly used area-length methods. The CMR measurements from two- and four-chamber views

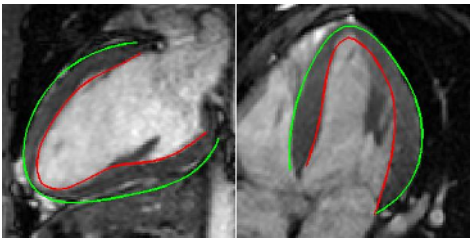

Fig. 6. Automatically detected myocardial endocardial (red) and epicardial (green) boundaries for two- (left) and four-chamber (right) view images

were polled together. The regression analysis was used to estimate the strength and direction of a linear relationship between manual and automatic measurements and graphically summarized in Fig.5. The paired t-test revealed statistically indistinguishable differences at 5% significance level between the manual and automatic segmentation for all parameters (two-chamber: EDV p=0.26; ESV p=0.09; EF p=0.1; four-chamber: EDV p=0.17; ESV p=0.34; LVM p=0.16) but two-chamber LVM (p=0.01) and four-chamber EF (p=0.04). The results of automatic segmentation are shown in Fig.6.

4 Discussion and Conclusions

Creation of the navigational environment required the classification of the input image into three profoundly distinct classes: air, blood, and myocardium. Although this assumption may not be necessary true for cardiac images where other anatomical structures, such as myocardial fat, are present. Nevertheless, due to the use of EM algorithm with greedy search heuristics this requirement can be easily incorporated by adding one extra class into the statistical segmentation scheme. However decision about the number of distinguishable classes presented in input images remains a challenging problem.

To take into account the complex LV geometry, three different sets of the navigational parameters were utilized depending on the LV region. However, the requirements for the robot navigation in the basal and midventricular regions can be combined together, resulting in only two sets of the navigational parameters. Further simplification of our method may be achieved by letting the robot navigate in only two segments (i.e. posterior and anterior myocardial walls starting from the mitral points towards the apex). Implementation of the aforementioned improvements would require accurate tracing of the mitral points in all phases because of the prominent cardiac contraction.

A better path planning procedure based on the "look-ahead" strategy resulted in a more robust navigation of the robot. A number of different paths is tried to determine the safest route, before the robot advances only one step forward. This results in increased computational demands and a slightly lower performance. An alternative approach would involve the map-based navigation

using the simulated topological maps of the navigational environment [11]. In this case the neighborhood around the robot's current positions would be matched against templates of the environment from the database and the precalculated path for the chosen template can be undertaken. However, it remains debatable whether the map-based navigation will be more computationally efficient.

Our validation study was carried out only on a group of healthy subjects. Some assumptions (i.e. the predefined myocardial wall thickness in the contour reconstruction phase) may not be valid for abnormal hypertrophic hearts. Hence, further validation of our method in patients is desirable.

In this paper an unorthodox method for the myocardial border detection in long-axis views using the adaptive exploring robot was presented. Using this approach a reliable and consistent segmentation of the myocardial boundary can be achieved. A clinical validation on a group of healthy subjects showed good agreement between the global LV function computed from manually and automatically segmented images.

Acknowledgement

Support of this research by the grant from Dutch Foundation for Technical Sciences (STW Project LPG 5651) is greatly appreciated. We express our gratitude to Dr. B. P. F. Lelieveldt for proof reading the manuscript.

References

1. A. Yezzi, S. Kichenassamy, A. Kumar, P. Olver, and A. Tannenbaum, "A geometric snake model for segmentation in medical imagery," *IEEE Trans. on Pattern Analysis and Machine Intelligence*, vol. 6, no. 2, pp. 199–209, 1997.
2. T. F. Cootes, G.J.Edwards, and C. J. Taylor, "Active appearance models," *IEEE Trans. on Pattern Analysis and Machine Intelligence*, vol. 23, no. 6, pp. 681–685, 2001.
3. C. R. Oost, B. P. F. Lelieveldt, M. Uzumcu, H. Lamb, J. H. C. Reiber, and M. Sonka, "Multi-view active appearance models: Application to x-ray lv angiography and cardiac mri," in *LNCS 2732*, 2003, pp. 234–245.
4. F. Admiraal-Behloul, B. P. F. Lelieveldt, L. Ferrarini, H. Olosfen, R. J. van der Geest, and J. H. C. Reiber, "A virtual exploring mobile robot for left ventricle contour tracking," in *Proc. IJCNN*, 2004, vol. 1, pp. 333–338.
5. A. P. Dempster, N. M. Laird, and D. B. Rubin, "Maximum likelihood from incomplete data via the em algorithm," *Journal of the Royal Statistical Society (B)*, vol. 39, no. 1, pp. 1–38, 1977.
6. X. Ye and J. A. Noble, "High resolution segmentation of mr images of mouse heart chambers based on a partial-pixel effect and em algorithm," in *Proc. ISBI*, 2002, pp. 257– 260.
7. J. J. Verbeek, N. Vlassis, and B. Krose, "Efficient greedy learning of gaussian mixture models," *Neural Computation*, vol. 15, no. 2, pp. 469–485, 2003.
8. S. Geman and D. Geman, "Stochastic relaxation, gibbs distributions, and the bayesian restoration of images," *IEEE Trans. On Pattern Analysis and Machine Intelligence*, vol. 6, no. 6, pp. 721–741, 1984.

9. V. Vezhnevets, "Method for localization of human faces in color based face detectors and trackers," in *Proc. ICDIPCES*, 2002, pp. 51–56.
10. M. Unser, "Splines - a perfect fit for signal/image processing," *IEEE Signal Processing Magazine*, vol. 16, no. 6, pp. 22–38, 1999.
11. G. N. DeSouza and A. C. Kak, "Vision for mobile robot navigation: A survey," *IEEE Trans. on Pattern Analysis and Machine Intelligence*, vol. 24, no. 2, pp. 237–267, 2002.